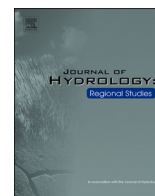





ELSEVIER

Contents lists available at [ScienceDirect](https://www.sciencedirect.com)

Journal of Hydrology: Regional Studies

journal homepage: www.elsevier.com/locate/ejrh

Land use land cover change, irrigation and their impacts on Bi-hourly evolution of convective environments during GRAINEX

Daniel Whitesel^{a,b}, Rezaul Mahmood^{a,b,*} , Paul Flanagan^c, Chris Phillips^d, Roger A. Pielke Sr.^{e,f}, Udaysankar Nair^d, Eric Rappin^g

^a High Plains Regional Climate Center, University of Nebraska-Lincoln, Lincoln, NE 68583, United States

^b School of Natural Resources, University of Nebraska-Lincoln, Lincoln, NE 68583, United States

^c US Department of Agriculture-Agricultural Research Service, El Reno, OK 73036, United States

^d Department of Atmospheric and Earth Science, University of Alabama in Huntsville, Huntsville, AL 35899, United States

^e Department of Atmospheric and Oceanic Sciences and University of Colorado-Boulder, Boulder, CO 80309, United States

^f Cooperative Institute for Research in Environmental Sciences, University of Colorado-Boulder, Boulder, CO 80309, United States

^g Kentucky Climate Center, Western Kentucky University, Bowling Green, KY 42101, United States

ARTICLE INFO

Keywords:

Convection

Land-atmosphere interactions

Agricultural impacts

ABSTRACT

Study Region: Eastern Nebraska, USA.

Study Focus: The objective of this research is to determine the impacts of irrigation on convective development. For this purpose, the study analyzed bi-hourly rawinsonde data collected during the Great Plains Irrigation Experiment for selected diagnostic variables during early and late growing season for cloudy and clear conditions. It was found that over irrigated land use observations recorded higher convective available potential energy and lower convective inhibition values compared to non-irrigated land use, along with lower dewpoint depressions. Irrigated land use also observed higher precipitable water during morning and clear days, while non-irrigated land use had higher values during the afternoon hours and non-clear days. A similar pattern can be seen for lapse rates for surface to 3 km, with observations over irrigated land use reported higher lapse rates during the morning and the evening hours and non-irrigated land use observing higher lapse rates during the afternoon hours. These factors, influenced by irrigated land use, contributed to a favorable convective environment during the morning and evening hours while non-irrigated land use provided a favorable convective environment during the afternoon hours.

New hydrological insights for the region: This research shows irrigation can impact development of convection, their timing, and hence potentially timing of precipitation. This finding can potentially assist in more efficient local and regional water resources management and planning.

1. Introduction

Land use land cover change (LULCC) impacts weather and climate (Pielke et al., 2011, 2016; Mahmood et al., 2010, 2013, 2014). These changes can be thermodynamic, such as changes in the surface energy balance and the hydrological cycle, and physical in nature such as changes in terrain, vegetation, and circulations (Mahmood et al., 2004, 2006, 2012; Pielke et al., 2011, 2016; Fan et al., 2015a, 2015b; Xu et al., 2015; Rappin et al., 2021; Phillips et al., 2022). Over the last couple of decades scientific community has placed a

* Corresponding author at: High Plains Regional Climate Center, University of Nebraska-Lincoln, Lincoln, NE 68583, United States.

E-mail address: rmahmood2@unl.edu (R. Mahmood).

<https://doi.org/10.1016/j.ejrh.2025.102884>

Received 5 January 2025; Received in revised form 15 September 2025; Accepted 24 October 2025

Available online 1 November 2025

2214-5818/© 2025 The Author(s). Published by Elsevier B.V. This is an open access article under the CC BY-NC-ND license (<http://creativecommons.org/licenses/by-nc-nd/4.0/>).

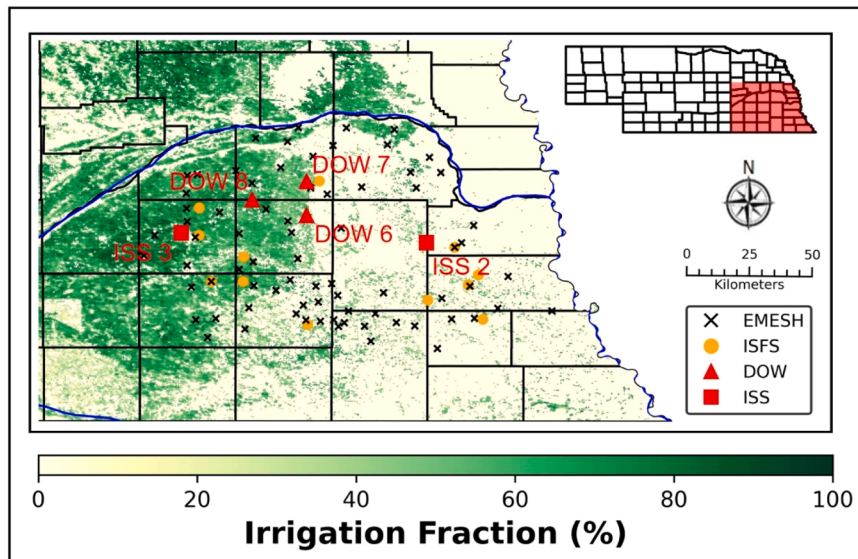


Fig. 1. Map of the GRAINEX study area in southeast Nebraska. Data collection sites consisted of 12 integrated surface flux system sites (ISFS), two integrated sounding system sites (ISS), three Doppler on Wheels deployment locations (DOW), and 75 Environmental Monitoring, Economical Sensor Hubs (EMESH). Rawinsondes (weather balloons) were launched from ISS and DOW sites (Source: Whitesel 2024b).

gradually increasing emphasis on the irrigation related LULCC and its impacts on the weather and climate. Changes in temperature, moisture, and regional circulations have been documented for regions that adopted irrigated agriculture (Barnston and Schickedanz, 1984; Mahmood and Hubbard, 2002; Mahmood et al., 2004, 2006, 2013; Cook et al., 2011, 2015, 2020; Sen Roy et al., 2007, 2011; DeAngelis et al., 2010; Pei et al., 2016; Szilagyi and Franz, 2020; McDermid et al., 2021, 2023; Rappin et al., 2021; Phillips et al., 2022; Brooke et al., 2023; Hu et al., 2024; Whitesel et al., 2024a). Surface temperatures and precipitation can be reduced in areas with widespread irrigation (Mahmood and Hubbard, 2002; Sen Roy et al., 2011; Barnston and Schickedanz, 1984; DeAngelis et al., 2010; Pei et al., 2016; Szilagyi and Franz, 2020). However, precipitation has been found to increase in areas downwind of the irrigated sites (Barnston and Schickedanz, 1984; DeAngelis et al., 2010; Pei et al., 2016; Greve et al., 2025).

For precipitation, development of convection is the key and, instability and moisture are two of the three main ingredients required for convection (Doswell et al., 1996; Brooks, 2007). Along with lift and shear, instability and moisture are used in a process called “ingredients based forecasting”, which determines if the ingredients are sufficient for convection to occur (Doswell et al., 1996). Variables that are used to assess instability are convective available potential energy (CAPE) (Moncrieff and Miller, 1976), convective inhibition (CIN) (Colby, 1984), Lifted Index (LI) (Galway, 1956), and environmental lapse rates (Carlson et al., 1983; Doswell et al., 1985; Craven and Brooks, 2004). Variables that are used to assess moisture include dewpoint depression ($DD_{850\text{ mb}}$) (Lewis, 1957) and precipitable water (PWAT) (Schultz, 1989; Salby, 1996). Typical operations at the National Weather Service of the United States involve sounding launches twice daily, once in the morning and once in the evening. An additional launch may be conducted, if necessary, during mid-day to assess the daytime state of the atmosphere, especially in environments predicted to favor the formation of severe convective storms. In other words, evolution of convective environment cannot be assessed in-between morning and evening soundings based on observational data. Moreover, in most, if not all, cases these soundings are not launched over an irrigated area.

Thus, lack of observational data with high spatio-temporal resolution is a weak point for the application of these diagnostic measures and improve our understanding of the impacts of irrigated land use on convective environment and its diurnal evolution. As a result, the overarching objective of this research was to investigate the daytime evolution of convective environment over irrigated and non-irrigated land use. For this purpose, the current study applied previously mentioned convective diagnostic variables to a large set of unique bi-hourly rawinsonde observations (40 per day = eight launches x five locations) collected over two 15 day periods (total 30 day; ~1200 launches = 40 launches per day x 30 day) during the Great Plains Irrigation Experiment (GRAINEX; Rappin et al., 2021) in Nebraska, USA in 2018 (Fig. 1). These balloon launches were conducted over irrigated, non-irrigated, and in-between transitional land uses to understand their impacts on the evolution of convective environment throughout the day. Specifically, diagnostic variables including CAPE, CIN, LI, 850 mb dewpoint depressions ($DD_{850\text{ mb}}$), PWAT, Surface – 3 km lapse rate, and 700 mb – 500 mb lapse rate, are used for all launches. Subsequently, calculated data for these diagnostic variables are analyzed in a bi-hourly interval from dawn until dusk for irrigated, non-irrigated, and in-between transitional land uses. These meteorological diagnostic variables also capture impacts of atmospheric changes in moisture and heat content due to changes in land surface hydrologic conditions caused by human intervention (e.g., irrigation). GRAINEX is the first field campaign focused on the impact of irrigation on convective environments. An added benefit of GRAINEX is that it allowed researchers to explore the impacts of a modified land surface hydrology (i.e., increased soil moisture and latent heat flux or ET over irrigated land use; in this paper we have used latent heat flux and ET interchangeably) on the convective environment. Overall, the results provide a better understanding of side-by-side evolution of convective

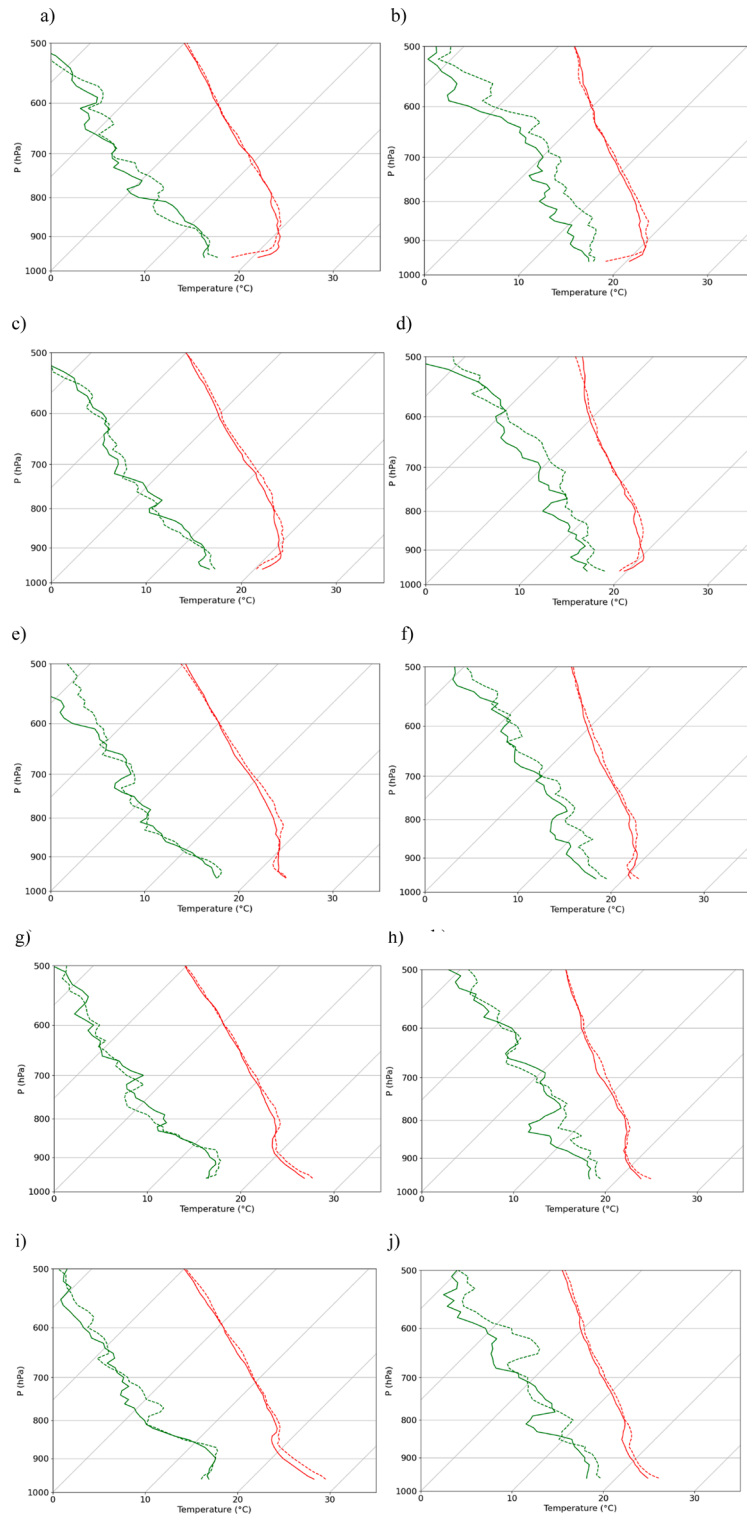


Fig. 2. Skew-T plots of average air temperature (red lines) and average dewpoint temperature (green lines) for non-irrigated ISS2 (solid) and irrigated ISS3 (dashed) for early (IOP1) (left) and peak (IOP2) growing season (right): a) 0500 LST (1100 UTC), IOP1; b) 0500 LST (1100 UTC), IOP2; c) 0700 LST (1300 UTC), IOP1; d) 0700 LST (1300 UTC), IOP2; e) 0900 LST (1500 UTC), IOP1; f) 0900 LST (1500 UTC), IOP2; g) 1100 LST (1700 UTC), IOP1; h) 1100 LST (1700 UTC), IOP2; i) 1300 LST (1900 UTC), IOP1; j) 1300 LST (1900 UTC), IOP2; k) 1500 LST (2100 UTC), IOP1; l) 1500 pm LST (2100 UTC), IOP2; m) 1700 LST (2300 UTC), IOP1; n) 1700 pm LST (2300 UTC), IOP2; o) 1900 LST (0100 UTC), IOP1; and p) 1900 LST (0100 UTC), IOP2.

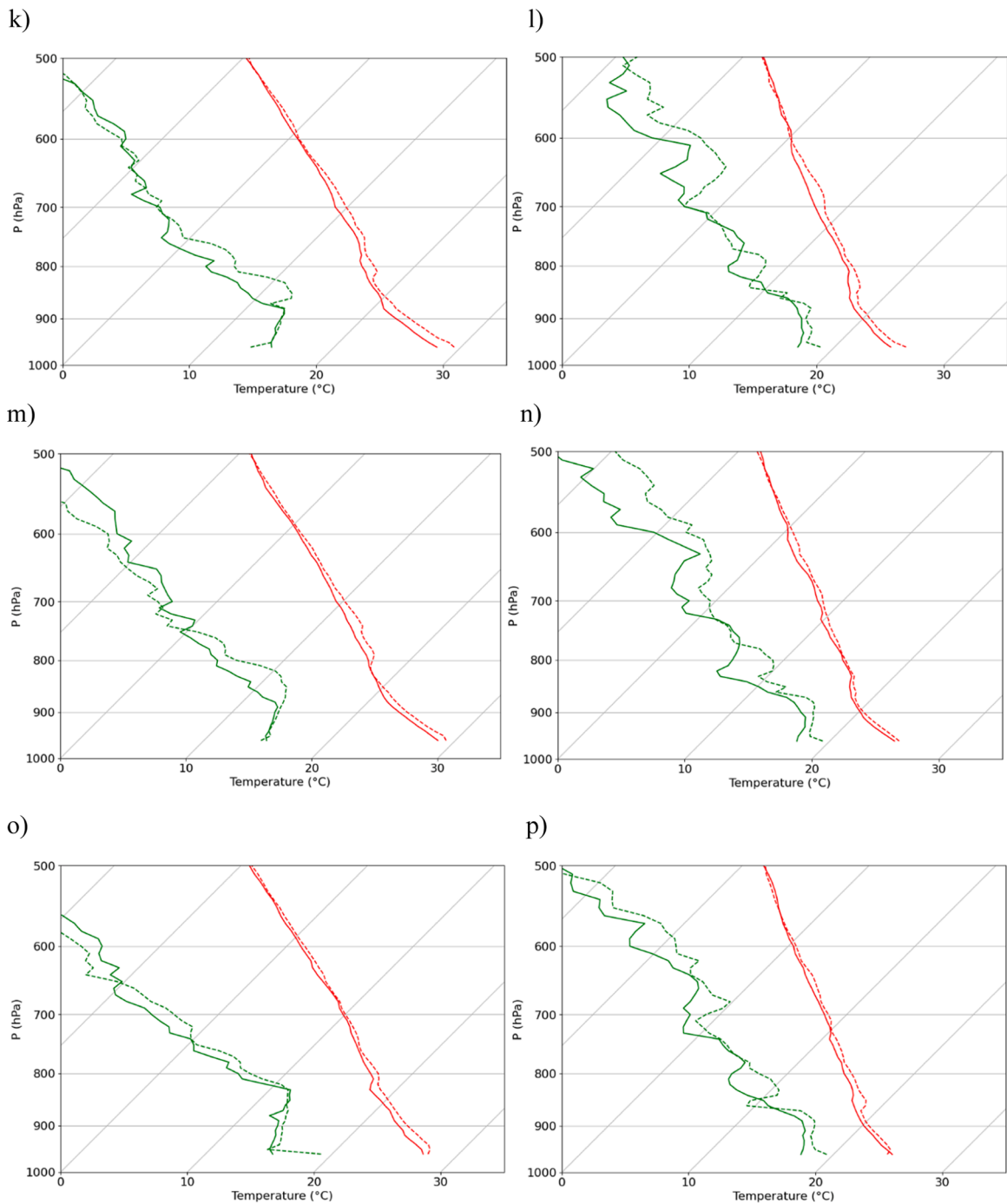


Fig. 2. (continued).

environments over two different land uses, including, irrigated and non-irrigated.

To provide further rationale for using the GRAINEX data in this research, a daytime evolution of air temperature and dewpoint temperature over an irrigated and a non-irrigated areas for the entire Intense Observation Period 1 [IOP1, which represents early crop growing season (May 30 to June 13)] and Intense Observation Period 2 [IOP2, which represents peak crop growing season (July 16-July 30)] is shown in Fig. 2a-p (n = ~1200 rawinsonde launches). Compared to non-irrigated land use, higher dewpoint temperature was found from surface to 500 mb for most of the day over irrigated areas, observed by rawinsonde launched from the Integrated Sounding System 3 (ISS3) during IOP2 (Fig. 2b, d, f, h, j, l, n, p, right panels). In other words, applications of irrigation made the atmosphere more moist during IOP2. Rawinsonde launched from over non-irrigated land use is identified as ISS2. In addition, the

transition from a stable boundary layer to a well-mixed convective boundary layer can be observed in the early afternoon to early evening hours for both sites and during both IOPs. Air temperature at the surface was lower for both sites in IOP2 compared to IOP1, and air temperature from the low to middle atmosphere appeared to decrease at a slower rate during IOP2 compared to IOP1. Fig. 2a-p, to the best of our knowledge, is the first where bi-hourly evolution of the atmospheric variables are shown over irrigated and non-irrigated land use during two different and complete periods (total 30 days) of growing seasons when irrigation applications vary notably.

Recently, Whitesel et al. (2025) conducted research focusing on irrigation impacts on convective environments by compositing data for morning and afternoon. The results suggest that further analysis of diagnostic variables by bi-hourly time-resolution is needed for better understanding of evolution of convective environments. This realization provided further motivation for the current research. Again, the availability of GRAINEX data assisted in addressing this need. The following sections presents data and methods, results and discussion, and conclusions.

2. Data and methodology

2.1. Data collection

Rawinsonde observations from two ISS (non-irrigated ISS2 and irrigated ISS3) (Parsons et al., 1994, UCAR/NCAR - Earth Observing Laboratory, 1997) and three Doppler on Wheels (DOW) (Wurman et al., 2021) sites (Fig. 1) were obtained during IOP1 (May 30, 2018, through June 13, 2018) and IOP2 (July 16, 2018, through July 30, 2018). The three DOW rawinsonde launching sites are identified as irrigated DOW8, non-irrigated DOW7 and transition zone DOW6. These land uses were determined based on the dataset developed by Ozdogan and Gutman (2008). These GRAINEX observation locations and associated land use were further verified by in-person site visits prior to the field campaign. Rawinsondes from all sites were launched simultaneously every two hours from 0500 am LST (1100 UTC) to 0700 pm LST (0100 UTC of the next day). The ISS sites launched a total of 480 balloons (8 launches x 2 sites x 30 days), and the DOW sites launched a total of 720 balloons (8 launches x 3 sites x 30 days). Thus, a total of about 1200 rawinsondes were launched during GRAINEX. The GRAINEX study area and the locations of various observation platforms that were used during the field campaign are shown Fig. 1. The other observation platforms used during GRAINEX include 12 Integrated Surface Flux System (ISFS) and 75 Environmental Monitoring Economical Sensor Hubs (EMESH). However, the observations collected by the ISFS and EMESH were not used for this paper. Data and results from these platforms are reported in Rappin et al. (2021) and Lachenmeier et al. (2024). Additional details about the field campaign can also be found in these papers (i.e., Rappin et al., 2021 and Lachenmeier et al., 2024).

2.2. Methodology

Summary of Calculated Diagnostic Variables

The diagnostic variables used for this paper are CAPE, CIN, LI, DD_{850 mb}, PWAT, and lapse rates from the surface – 3 km, and 700 mb – 500 mb. These diagnostic variables are proven tools for thunderstorm forecasts (Moncrieff and Miller, 1976; Colby, 1984; Carlson et al., 1983; Doswell et al., 1985, Salby, 1996; Craven and Brooks, 2004; Thompson, 2006).

CAPE quantifies the energy a lifted parcel carries as it ascends into the atmosphere (Moncrieff and Miller, 1976). CIN quantifies the energy required to lift a parcel to the Level of Free Convection (LFC) (Colby, 1984). Both CAPE and CIN can be expressed as follows (May et al., 2022, 2024):

$$CAPE = -R_d \int_{LFC}^{EL} (T_{v_{parcel}} - T_{v_{environment}}) d\ln p \quad (1)$$

$$CIN = -R_d \int_{SFC}^{LFC} (T_{v_{parcel}} - T_{v_{environment}}) d\ln p \quad (2)$$

These equations are generally similar, but the limits of integration are different, with the CAPE ranging from the LFC to the equilibrium level (EL) and the CIN ranging from the surface to the LFC. The LI is the difference between a parcel's temperature at 500 mb and the environmental temperature at 500 mb, shown below (May et al., 2022, 2024):

$$LI = T_{500mb} - T_{500mb_{parcel}} \quad (3)$$

DD_{850 mb} is the difference between the air temperature and dewpoint temperature at a given pressure level and it was calculated for 850 mb (Lewis, 1957). Dew point temperature is a measure of atmospheric moistness. When the difference between the air temperature and dewpoint temperature is low, it suggests a more moist atmosphere. The precipitable water (PWAT) was calculated from the surface to 500 mb. The PWAT can be expressed as follows (May et al., 2022, 2024):

$$PWAT = - \frac{1}{\rho_v g} \int_{SFC}^{500mb} r dp \quad (4)$$

where PWAT is the integral of the water vapor mixing ratio with respect to pressure. Finally, environmental lapse rates were calculated for two different layers: surface – 3 km and 700 mb – 500 mb levels. These lapse rates are used regularly at the Storm Prediction Center (Storm Prediction Center, 2024) and importance has been placed on the 700 mb – 500 mb lapse rate for severe weather forecasting

Table 1

Average LI, PWAT, DD_{850 mb}, and surface – 3 km lapse rates by rawinsonde launch time and by IOP for all sites. All times are local standard time. Statistical significance tests were completed using a 95 % confidence interval (p < 0.05) for the following: Irrigated ISS3 vs Non-Irrigated ISS2 (**Bold**), Irrigated ISS3 vs. Transitional DOW6 (*Italic*), Irrigated ISS3 vs. Non-Irrigated DOW7 (*), and Irrigated DOW8 vs Non-Irrigated ISS2 (+). Respective symbols represent statistically significant results. For brevity, significance tests were not completed for all possible combinations.

IOP1		0500	0700	0900	1100	1300	1500	1700	1900
ISS2	LI	2.2	-0.9	-2.9	-3.5 ⁺	-4.2 ⁺	-3.8 ⁺	-3.3 ⁺	-3.0
	PWAT	27.9	27.9 ⁺	27.3 ⁺	28.4 ⁺	28.2 ⁺	28.9 ⁺	30.0	30.2 ⁺
	DD _{850 mb}	9.9	9.7	12.3	9.8	8.9	10.2	10.4	7.1
	Γ _{SFC-3KM}	3.9	4.8	5.9 ⁺	6.5	6.8	7.1	7.1	6.0⁺
ISS3	LI	1.4	-1.3*	-3.6*	-3.6*	-3.5*	-3.5*	-4.0*	-3.9*
	PWAT	26.1	25.9	25.9	26.8	27.5	28.5	28.1	28.5
	DD _{850 mb}	12.3	11.9	12.3	10.0	10.3	7.1	7.7	8.0
	Γ _{SFC-3KM}	4.1	4.8	5.8	6.5	7.0	7.2	7.5	6.7
DOW6	LI	1.7	<i>0.8</i>	<i>-1.0</i>	<i>-1.3</i>	<i>-1.7</i>	<i>-1.7</i>	<i>-1.8</i>	<i>-1.4</i>
	PWAT	27.7	26.0	25.8	26.3	26.6	28.1	28.5	28.3
	DD _{850 mb}	10.0	12.4	12.0	9.6	8.5	9.3	7.7	7.4
	Γ _{SFC-3KM}	4.3	4.7	5.7	6.3	6.8	7.2	7.1	6.5
DOW7	LI	1.3	-0.7*	-1.4*	-1.5*	-1.7*	-1.1*	-1.3*	-0.7*
	PWAT	24.3	25.6	25.3	26.4	26.4	27.9	27.6	27.1
	DD _{850 mb}	9.4	11.5	11.2	8.8	8.3	9.5	9.6	8.1
	Γ _{SFC-3KM}	4.1	5.0	5.8	6.5	6.9	7.2	7.0	6.6
DOW8	LI	1.7	-0.2	-2.2	-2.3 ⁺	-2.1 ⁺	-1.4 ⁺	-2.4 ⁺	-2.2
	PWAT	26.1	24.8 ⁺	25.1 ⁺	26.3 ⁺	26.2 ⁺	27.3 ⁺	27.9	28.5 ⁺
	DD _{850 mb}	10.0	10.9	12.0	9.2	9.1	8.8	8.3	7.4
	Γ _{SFC-3KM}	4.1	4.7	5.8 ⁺	6.6	6.9	7.2	7.1	6.6 ⁺
IOP2		0500	0700	0900	1100	1300	1500	1700	1900
ISS2	LI	3.8⁺	0.8	-1.1	-1.7 ⁺	-2.5 ⁺	-2.9 ⁺	-3.3 ⁺	-2.9
	PWAT	31.7	32.3	32.8	33.2	32.9 ⁺	34.1 ⁺	33.4	33.2
	DD _{850 mb}	9.0 ⁺	7.1	8.3	8.0	5.5	6.5	7.1	7.0
	Γ _{SFC-3KM}	3.7⁺	4.4	5.5	6.2	6.4	6.7	6.6	5.9
ISS3	LI	1.7	0.3*	-0.9*	-2.8*	-3.4*	-4.3*	-4.5*	-3.8*
	PWAT	33.6*	33.5*	33.6*	33.6*	33.2*	33.5*	34.6*	33.4*
	DD _{850 mb}	6.2	5.9	4.7	6.1	7.9	5.5	5.3	9.1
	Γ _{SFC-3KM}	4.1	4.7	5.4	6.0	6.3	6.3	6.3*	5.8*
DOW6	LI	2.5	1.8	0.0	-0.9	-0.9	-2.0	-1.9	-2.8
	PWAT	31.3	31.2	31.9	31.0	32.5	32.2	31.7	30.2
	DD _{850 mb}	6.2	7.0	6.8	7.5	6.7	6.7	6.9	9.3
	Γ _{SFC-3KM}	4.3	4.6	5.5	6.0	6.3	6.3	6.5	6.1
DOW7	LI	3.3	2.3*	0.2*	-0.7*	-0.5*	-1.7*	-2.3*	-2.6*
	PWAT	31.5*	32.0*	31.0*	30.7*	31.1*	31.9*	30.7*	30.7*
	DD _{850 mb}	6.2	6.6	6.8	7.8	8.2	6.3	7.2	9.4
	Γ _{SFC-3KM}	4.1	4.6	5.5	6.1	6.3	6.5	6.6*	6.1*
DOW8	LI	1.6 ⁺	1.2	-0.5	-0.2 ⁺	-0.9 ⁺	-1.7 ⁺	-2.4 ⁺	-2.9
	PWAT	32.5	31.5	32.5	31.5	31.9 ⁺	32.6 ⁺	32.4	32.1
	DD _{850 mb}	5.0 ⁺	5.4	6.1	6.9	5.9	6.3	7.7	8.5
	Γ _{SFC-3KM}	4.2 ⁺	4.5	5.4	5.9	6.3	6.3	6.5	6.1

(Carlson et al., 1983; Doswell et al., 1985; Lanicci, 1985; Lanicci and Warner, 1991a, b, c; Craven and Brooks, 2004).

2.3. Data analysis

The above-mentioned diagnostic variables were calculated for every launched sounding from all five rawinsonde launch sites representing irrigated, non-irrigated, and transitional land use. The timeseries generated for each diagnostic variables were then sorted by the time of launch, land use and were separated by IOP (IOP1 and IOP2), cloud cover (clear and non-clear days), and by IOP and cloud cover together. Clear days represent when solar forcing is substantial and larger scale synoptic forcing is minimal while land use land cover and irrigation and resulting increased soil moisture impacts on atmosphere would be strong. On the other hand, cloudy days suggest both synoptic influences along with land use land cover and irrigation impacts. The main idea of these categorizations is to show the impacts of irrigated and non-irrigated land uses and associated land surface hydrologic conditions on the diurnal evolution of the selected variables first during IOP1 and IOP2, then by clear and non-clear days, and finally during clear days in IOP1 and IOP2, and non-clear days in IOP1 and IOP2. These categorizations were successfully used in Lachenmeier et al. (2024) and Whitesel et al. (2024b). Subsequently, means were calculated for each diagnostic variable (e.g., LI, CIN etc.) for each launching time and under various categories (e.g., IOP1, IOP2, cloudy day, non-cloudy day etc.). Statistical significance tests were also completed by comparing these values for irrigated and non-irrigated land use. Further details on the data analysis can be found in the following section.

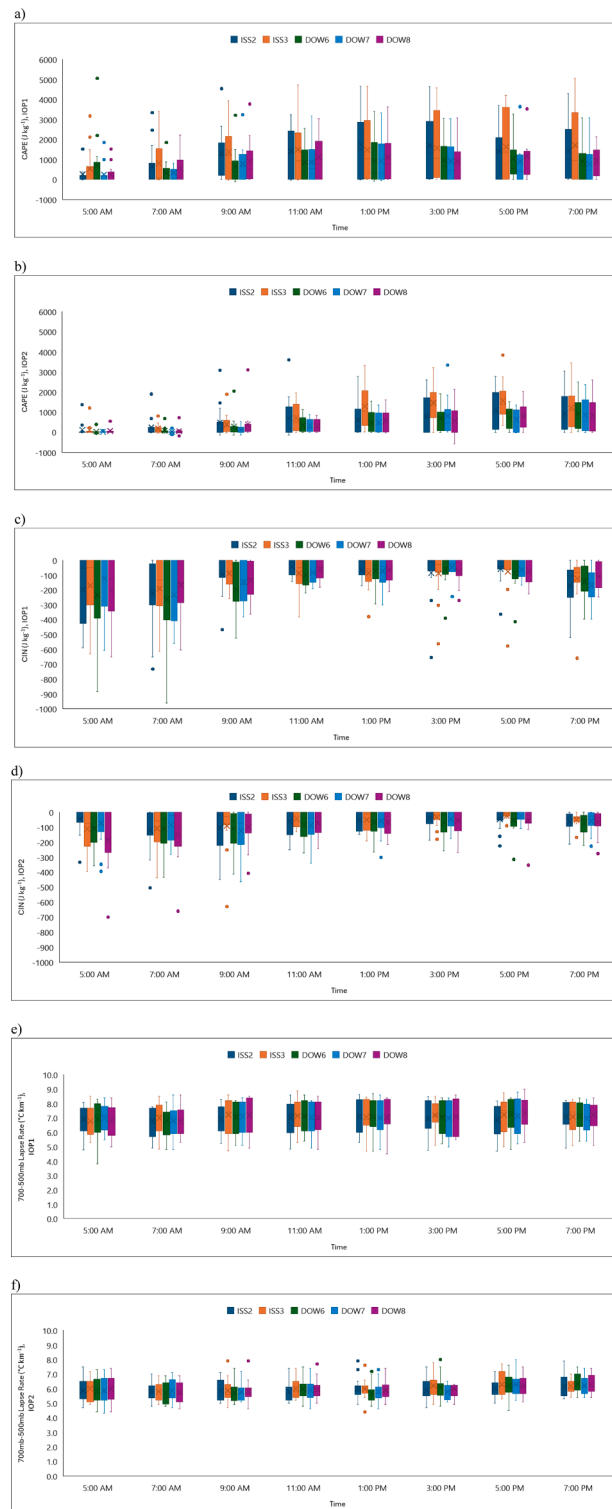


Fig. 3. Box and whisker plots of: a) CAPE, IOP1; b) CAPE, IOP2; c) CIN, IOP1; d) CIN, IOP2; e) 700 mb – 500 mb lapse rate, IOP1; and f) 700 mb – 500 mb lapse rate, IOP2. All times are local standard time.

3. Results and discussion

3.1. Results

3.1.1. IOP

Table 1 shows average LI, PWAT, $DD_{850\text{ mb}}$, and the surface – 3 km environmental lapse rates for all sites by IOP by every two-hour when a rawinsonde was launched. During IOP1, average LI values for irrigated area ISS3 (non-irrigated area ISS2) ranged from -4.0 – 1.4 °C

(-4.2 – 2.2 °C) for the eight daily observation period (Table 1), with the lowest LI values observed at 0900, 1100, 1700, 1900 LST (1300 and 1500 LST) launch times. During IOP2, irrigated ISS3 (non-irrigated ISS2) observed average LI values ranged from -4.5 – 1.7 °C (-3.3 – 3.8 °C) for the eight daily observation period (Table 1). The lowest LI values were typically observed between 1500 and 1900 LST launches for both irrigated ISS3 and non-irrigated ISS2.

For all sites, average PWAT increased from IOP1 to IOP2 suggesting moistening of the atmosphere linked to higher latent heat flux from increased irrigation and growing crop fields. For example, at irrigated ISS3 (non-irrigated ISS2) during IOP1 observed average PWAT values ranged from 25.9 to 28.5 mm (27.3–30.2 mm) for eight daily launch times (0500, 0700, 0900, 1100, 1300, 1500, 1700, and 1900 LST rawinsonde launch times, respectively) (Table 1). ISS3 reported up to 2.0 mm less PWAT than ISS2 during IOP1 for a given launch time. Absence or limited irrigation during IOP1 (early growing season) over irrigated areas resulted in these lower PWAT values. However, during IOP2, the irrigated ISS3 site observed up to 8.7 mm higher PWAT values compared to IOP1 and up to 2.9 mm higher compared to over the non-irrigated ISS2 site during IOP2, for the previously mentioned observation times (Table 1).

Again, increased irrigation, moist land surface conditions, and a relatively higher latent heat flux during IOP2 (peak growing season) played an important role in this increase (cf., Rappin et al., 2021; Lachenmeier et al., 2024; Whitesel et al., 2024b). Irrigation and resulting wetter soils support a positive soil moisture–convection feedback where the PBL moistens resulting from an increased latent heat flux (Eltahir, 1998; Findell and Eltahir 2003a,b; Collow et al., 2014; Santanello et al., 2018; Lachenmeier et al., 2024; Whitesel et al., 2024b). Soil moisture modifies the surface energy and water budgets through changes of albedo and the Bowen ratio (the ratio of the surface sensible heat flux to the latent heat flux, or ET) or the evaporative fraction [EF, the ratio of the latent heat flux to the net surface flux (i.e., net radiative flux)] (Whitesel et al., 2024b). In other words, in the current research, wetter soils partitioned larger amounts of incoming solar radiation to latent heat flux/ET. This led to a relatively smaller sensible heat flux and a larger EF, which positively impacted PWAT.

These understandings are further supported by McPherson (2007) who noted that the strength of land–atmosphere interactions is sensitive to soil moisture. Along this line, Holt et al. (2006) previously suggested that soil moisture changes (caused by irrigation) affect L–A interactions due to modifications in the sensible and latent energy (or ET) partitioning, air temperature, and PBL moisture content. They also indicated that atmospheric response to these changes propagates upward through the boundary layer via turbulent transport and affects boundary layer growth, convective initiation, and precipitation amounts. Changes observed in the current study resulted from similar atmospheric responses linked to higher soil moisture content caused by irrigation.

Average dew point depression ($DD_{850\text{ mb}}$) decreased from IOP1 to IOP2 for all sites, which suggests moistening of the atmosphere due to irrigation (moist land surface hydrologic condition). For example, the non-irrigated ISS2 site during IOP1 observed average $DD_{850\text{ mb}}$ values ranged between 7.1 and 12.3 °C for the eight daily observation period (Table 1). While during IOP2, an average $DD_{850\text{ mb}}$ value decreased noticeably, compared to IOP1. During IOP2, an observed average $DD_{850\text{ mb}}$ over irrigated ISS3 ranged between 4.7 and 9.1 °C and they were up to 4.3 °C lower compared to non-irrigated ISS2 (Table 1). It is previously (Section 2.2) noted that lower $DD_{850\text{ mb}}$ indicates a more moist atmosphere. Hence, these lower $DD_{850\text{ mb}}$ values at the irrigated ISS3 during IOP2 (peak growing season) and when compared to non-irrigated ISS2, suggest a more moist atmosphere. This occurred due to increased soil moisture and latent heat flux linked to increased irrigation and an altered land surface hydrologic condition.

Surface – 3 km lapse rates for irrigated ISS3 during IOP1 ranged between 4.1 and 7.5 °C km⁻¹ and they increased throughout the day (Table 1). During IOP2, they ranged between 4.1 and 6.3 °C km⁻¹ (Table 1). Overall, surface – 3 km lapse rates for the ISS3 site decreased by up to 1.2 °C km⁻¹ compared to IOP1. During IOP2, average observed surface – 3 km lapse rates for non-irrigated ISS2 ranged between 3.7 and 6.7 °C km⁻¹ and these values increased throughout the day (Table 1). In addition, these lapse rates were higher than ISS3 for most observation times except in the early morning (Table 1).

Observations from irrigated DOW8 and non-irrigated DOW7 show results that are generally similar to results from irrigated ISS3 and non-irrigated ISS2 (Table 1). While, as expected, DOW6 shows results that are somewhat representative of transitional land use between irrigated and non-irrigated. For the sake of brevity detailed discussion on the findings from irrigated DOW8, non-irrigated DOW7, and transitional land use DOW6 is not provided here.

Fig. 3a-f shows the box and whisker plots of CAPE, CIN, and 700 mb – 500 mb lapse rates for IOP1 and IOP2. Observations suggest that average CAPE has decreased from IOP1 to IOP2 for all sites. For example, during IOP1, mean CAPE values for the irrigated ISS3 ranged between 530 and 1708 J kg⁻¹ (Fig. 3a). During IOP2, ISS3 reported mean CAPE values between 110 and 1576 J kg⁻¹ (Fig. 3b). While for IOP2, non-irrigated ISS2 reported average CAPE values between 119 and 1110 J kg⁻¹ for eight daily rawinsonde launch times (Fig. 3a-b). Compared to irrigated ISS3, the morning values were slightly higher for non-irrigated ISS2 (a 9, 54, 91, and 14 J kg⁻¹ difference), but irrigated ISS3 observed higher values of CAPE compared to over non-irrigated ISS2 during the afternoon hours (a 676, 667, 446, and 287 J kg⁻¹ difference).

Average CIN values for the irrigated ISS3 site during IOP1 ranged between -76 and -190 (Fig. 3c). During IOP2, they ranged between -24 and -110 J kg⁻¹ (up to 59 J kg⁻¹ higher compared to IOP1) (Fig. 3d). In other words, conditions for convection development became more favorable over irrigated land use during IOP2 when irrigation was in full swing. Average CIN values during

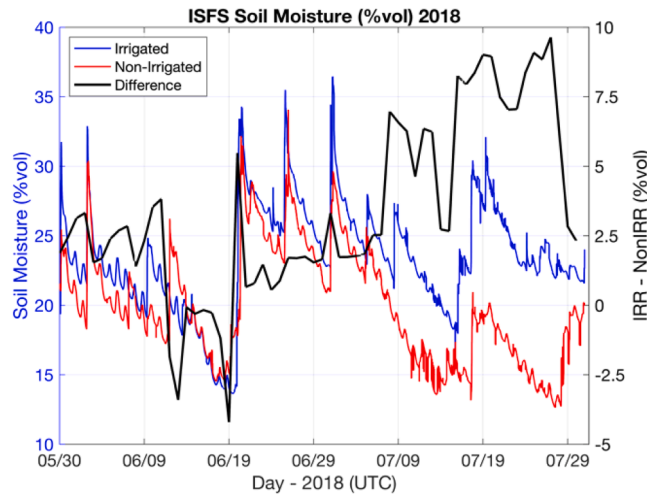


Fig. 4. Soil moisture for six irrigated and six non-irrigated ISFS sites (shown in Fig. 1) from May 30 to July 30, 2018. This figure includes early growing season (IOP1), peak growing season (IOP2), and the period in-between IOP1 and IOP2. Differences in soil moisture between irrigated and non-irrigated sites are present by the black line. Soil moisture difference continued to increase after June 19, as irrigation applications increased (Source: Rappin et al# 2021).

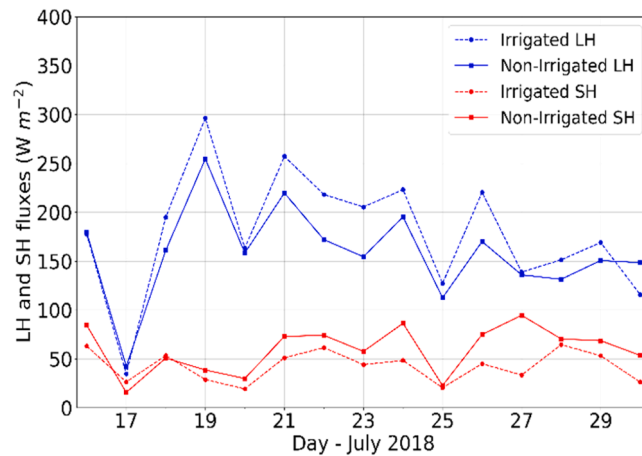


Fig. 5. Latent and sensible heat flux from irrigated and non-irrigated land use during IOP2 (peak growing season) (Source: Rappin et al# 2021).

IOP2 for the non-irrigated ISS2 site were up to 65 J kg^{-1} higher compared to irrigated ISS3 (Fig. 3d). Average 700 mb – 500 mb lapse rates for over irrigated ISS3 ranged between 6.8 and $7.2 \text{ }^\circ\text{C km}^{-1}$ for the observation times (Fig. 3e). During IOP2, they were up to $1.3 \text{ }^\circ\text{C km}^{-1}$ lower compared to IOP1 (Fig. 3f). The non-irrigated ISS2 found up to $0.3 \text{ }^\circ\text{C km}^{-1}$ lower lapse rates compared to ISS3 (Fig. 3f).

Overall, the transition from early (IOP1) to peak (IOP2) growing season has the largest effect on the magnitudes of all diagnostic variables analyzed. For example, CAPE, $DD_{850 \text{ mb}}$, and lapse rates from the surface – 3 km, and 700 mb – 500 mb have decreased from IOP1 to IOP2 for all sites. However, CAPE is higher over irrigated ISS3 and DOW8 compared to non-irrigated ISS2 and DOW7 and transition zone DOW6 during peak growing season (IOP2). Recall that irrigation increased notably during IOP2, which led to increased soil moisture (Fig. 4).

The decreases in environmental lapse rates at all levels appear to reflect another important change with the transition from IOP1 to IOP2. This decrease in lapse rate implies decreases in surface temperatures or increases in upper air temperatures or both when comparing IOP1 to IOP2. Note that Lachenmeier et al. (2024) has shown that surface temperature was lower over irrigated areas during GRAINEX due to higher latent and lower sensible heat flux linked to higher soil moisture and thus changed land surface hydrology (Figs. 4 and 5).

In addition, when dewpoint temperatures increase, dewpoint depression decreases given little or no change in air temperature as was the case during IOP2. As noted previously, it is an indication moistening of atmosphere during IOP2 around irrigated ISS3 due to increased irrigation, soil moisture content (Fig. 4), and latent heat flux (Fig. 5). Precipitable water (PWAT) increased from IOP1 to IOP2 due to increases in irrigation and simultaneous increases in soil moisture and latent heat flux. Overall, compared to non-irrigated

Table 2

Average LI, PWAT, DD_{850 mb}, and surface – 3 km lapse rates by rawinsonde launch time and by cloud cover for all sites. All times are local standard time. Statistical significance tests were completed using a 95 % confidence interval ($p < 0.05$) for the following: Irrigated ISS3 vs. Non-Irrigated ISS2 (**Bold**), Irrigated ISS3 vs. Transitional DOW6 (*Italic*), Irrigated ISS3 vs. Non-Irrigated DOW7 (*), and Irrigated DOW8 vs. Non-Irrigated ISS2 (+). Respective symbols represent statistically significant results. For brevity, significance tests were not completed for all possible combinations.

Clear		0500	0700	0900	1100	1300	1500	1700	1900
ISS2	LI	3.9	1.2	-1.1	-1.4	-1.6 ⁺	-1.5 ⁺	-1.2	-1.3
	PWAT	27.5	27.5	26.6	26.6	26.4	25.4	26.9	25.7
	DD _{850 mb}	11.6	10.1	12.2	12.1	9.3	11.1	11.3	11.8
	$\Gamma_{\text{SFC}-3\text{KM}}$	3.4	4.3	5.4	6.3	6.6	6.8	6.7	5.9 ⁺
ISS3	LI	3.8	1.4	-0.7*	-1.2*	-1.3	-1.9*	-2.6*	-3.1*
	PWAT	28.5	26.6	26.6	25.6	25.8	27.1	27.6	27.5*
	DD _{850 mb}	9.2	10.1	8.5	11.4	11.9	9.3	9.8	14.2
	$\Gamma_{\text{SFC}-3\text{KM}}$	3.5	4.4	5.5	6.0	6.3	6.7	7.0	6.4
DOW6	LI	5.0	2.8	0.9	0.4	0.6	0.1	0.1	-0.6
	PWAT	26.2	27.3	25.8	24.5	24.4	25.9	25.6	25.2
	DD _{850 mb}	7.5	10.1	10.6	11.1	10.0	9.6	11.6	15.4
	$\Gamma_{\text{SFC}-3\text{KM}}$	3.7	4.3	5.4	6.1	6.4	6.8	6.7	6.3
DOW7	LI	4.3	3.5	0.9*	0.0*	0.7	1.5*	0.1*	-0.4*
	PWAT	22.9	26.5	25.4	24.8	24.0	26.0	24.9	24.7*
	DD _{850 mb}	7.3	9.8	10.2	10.5	12.9	9.8	11.7	14.6
	$\Gamma_{\text{SFC}-3\text{KM}}$	3.7	4.5	5.5	6.1	6.4	6.7	6.8	6.4
DOW8	LI	3.0	1.7	-0.2	-0.3	0.0 ⁺	-0.2 ⁺	-0.6	-1.0
	PWAT	27.2	26.8	26.4	24.4	25.0	26.0	26.3	25.9
	DD _{850 mb}	7.8	8.3	10.1	10.7	8.9	9.6	12.6	13.8
	$\Gamma_{\text{SFC}-3\text{KM}}$	3.7	4.3	5.5	6.2	6.5	6.8	6.8	6.4 ⁺
Non-Clear		0500	0700	0900	1100	1300	1500	1700	1900
ISS2	LI	2.6 ⁺	-0.7	-2.4	-3.1 ⁺	-4.1 ⁺	-4.1 ⁺	-4.2 ⁺	-3.7
	PWAT	30.9	31.2 ⁺	31.5 ⁺	32.7 ⁺	32.8 ⁺	33.5 ⁺	33.8 ⁺	34.2 ⁺
	DD _{850 mb}	8.7	7.8	9.4	7.6	6.5	7.4	7.8	5.0
	$\Gamma_{\text{SFC}-3\text{KM}}$	3.9 ⁺	4.7	5.8	6.3	6.6 ⁺	6.9	6.9	5.9 ⁺
ISS3	LI	0.6*	-1.3*	-2.9*	-4.0*	-4.3*	-4.7*	-4.9*	-4.2*
	PWAT	30.7	31.0*	31.1*	32.2*	32.3*	32.7*	32.9	32.4
	DD _{850 mb}	9.1	8.4	8.5	6.7	8.0	5.3	5.4	6.1
	$\Gamma_{\text{SFC}-3\text{KM}}$	4.4	4.9	5.6	6.3	6.8	6.8	6.9	6.2
DOW6	LI	1.1	0.7	-1.2	-1.8	-2.1	-2.8	-2.8	-2.9
	PWAT	30.5	29.0	30.1	30.4	31.7	32.0	32.3	31.5
	DD _{850 mb}	8.6	9.4	9.1	7.5	6.8	7.6	5.6	4.9
	$\Gamma_{\text{SFC}-3\text{KM}}$	4.5	4.8	5.7	6.2	6.6	6.8	6.8	6.2
DOW7	LI	1.9*	0.7*	-1.4*	-1.7*	-1.9*	-2.5*	-2.6*	-2.2*
	PWAT	29.9	29.7*	29.3*	30.1*	30.7*	31.2*	31.2	30.9
	DD _{850 mb}	8.6	9.2	9.0	7.4	6.4	7.4	7.2	6.0
	$\Gamma_{\text{SFC}-3\text{KM}}$	4.3	4.9	5.7	6.4	6.7	6.9	6.7	6.3
DOW8	LI	1.1 ⁺	-0.1	-1.9	-1.7 ⁺	-2.3 ⁺	-2.2 ⁺	-3.3 ⁺	-3.3
	PWAT	30.3	28.6 ⁺	29.8 ⁺	30.8 ⁺	30.7 ⁺	31.6 ⁺	31.9 ⁺	32.6 ⁺
	DD _{850 mb}	7.9	8.4	8.8	6.9	7.1	6.9	5.9	5.2
	$\Gamma_{\text{SFC}-3\text{KM}}$	4.3 ⁺	4.8	5.6	6.3	6.7 ⁺	6.7	6.8	6.3 ⁺

areas, PWAT was higher, and dewpoint depression was lower over irrigated areas during IOP2. The timing of the highest average values of diagnostic variables have also changed with the progression of the IOPs. For example, average CAPE for the non-irrigated (irrigated) ISS2 (ISS3) site peaked to 1750 J kg⁻¹ (1708 J kg⁻¹) at 1300 LST (1900 LST) during IOP1 but peaked to 1110 J kg⁻¹ (1576 J kg⁻¹) at 1700 LST (1800 LST) during IOP2 (Table 1).

Previous studies using the GRAINEX surface data found soil moisture heterogeneity between irrigated and non-irrigated land use, where irrigated agriculture observed higher soil moisture (Fig. 4) (Rappin et al., 2021, 2022).

Impacts of the increased soil moisture were also observed in latent and sensible heat flux data. When compared to non-irrigated land use, irrigated land use shows consistently higher and lower latent and sensible flux, respectively, during IOP2 (peak growing season) (Fig. 5). This finding also fits with the understanding that plentiful water and a moist environment enhance latent heat flux. The current study suggests that human intervention via irrigation increased regional soil moisture content and created soil moisture heterogeneity between irrigated and non-irrigated land use, which eventually impacted latent and sensible heat fluxes over these two different land uses. The changes in fluxes further impacted the turbulent transfer of moisture and heat in the atmosphere, which influenced convective environment.

In addition, soil moisture heterogeneities can play an important role in convective initiation (Pielke, Zeng, 1989; Pielke, 2001; Findell and Eltahir, 2003a, b; Frye and Mote 2010a, b; Taylor et al., 2012, 2018; Lachenmeier et al., 2024; Whitesel et al., 2024 a, b; Paccini and Schiro, 2025). It has been shown that land surface hydrology and soil moisture differences can affect diagnostic variables such as CAPE and LI (Pielke, Zeng, 1989; Pielke, 2001; Frye and Mote, 2010b). In other words, increasing irrigation, and the resulting higher soils moisture (i.e., higher latent heat flux), can impact CAPE and LI and thus the convective environment. In this study, LI further decreased (larger negative) during IOP2 as irrigation increased, which suggests a more conducive convective environment.

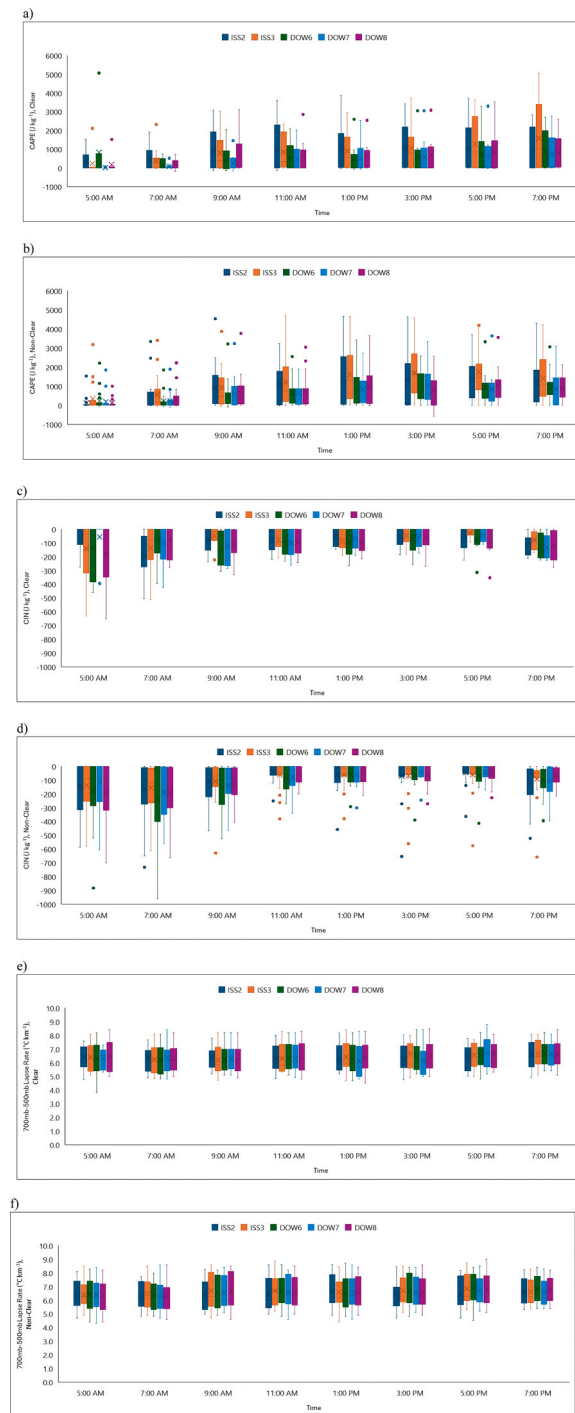


Fig. 6. a-f: Box and whisker plots of: a) CAPE, clear days, b) CAPE, non-clear days, c) CIN, clear days, d) CIN, non-clear days, e) 700 mb – 500 mb lapse rate, clear days, and f) 700 mb – 500 mb lapse rate, non-clear days. All times are local standard time.

Compared to IOP1, during IOP2, CAPE declined for both irrigated and non-irrigated land uses. This decrease in CAPE is primarily linked to the lowering of lapse rates (Fig. 2) due to the steady warming of the entire atmospheric column during IOP2 (July). However, CAPE was much greater over irrigated areas compared to non-irrigated during IOP2, suggesting an influence of increased soil moisture linked to irrigation. It is also found that irrigation/increased latent heat flux resulted in decrease of the Lifting Condensation Level (LCL), and the Level of Free Convection (LFC) (Lachenmeier et al., 2024) and hence, an increased favorability of convection. Overall,

the findings of this study are consistent with theoretical understanding of the role of increased soil moisture and latent heat flux due to irrigation and their impacts on convection.

3.1.2. Cloud Cover (Clear and non-clear days)

Table 2 shows the means of LI, PWAT, dewpoint depression at 850 mb ($DD_{850\text{ mb}}$), and the surface - 3 km environmental lapse rates for all sites by cloud cover (clear and non-clear days). Here, we did not separate data by IOPs. During clear days, average LI values for the irrigated ISS3 (non-irrigated ISS2) site ranged from -3.1 – -3.8 °C (-1.6 – -3.9 °C) for the eight daily rawinsonde launch periods (Table 2), with the lowest LI values being observed for the 1700 and 1900 LST (1300 and 1500 LST) launch times for the irrigated ISS3 (non-irrigated ISS2) site. However, during non-clear days, average LI values for the irrigated ISS3 (non-irrigated ISS2) site ranged from -4.9 – -0.6 °C (-4.2 – -2.6 °C) for the eight rawinsonde launches (Table 2). The lowest average LI values were typically observed for 1500 LST and 1700 LST (1300 through 1900 LST) launch times for the irrigated ISS3 (non-irrigated ISS2) site. Thus, under both clear and non-clear days irrigation provided conditions more favorable for convection development.

Average PWAT values for the irrigated ISS3 (non-irrigated ISS2) site ranged from 25.6 to 28.5 mm (25.4–27.5 mm) for clear days and eight daily launches, with the highest PWAT values being observed at 0500 LST launch times for both sites (Table 2). During non-clear days, average PWAT values for the irrigated ISS3 (non-irrigated ISS2) site ranged between 30.7 and 32.9 mm (30.9 and 34.2 mm) for the eight daily launch period, with the highest PWAT values being observed at 1300 LST (1900 LST) launch time. Hence, under clear conditions PWAT was distinctly higher over irrigated land use compared to over non-irrigated. Based on the average PWAT value, irrigated land use provides more favorable convective development conditions during clear days.

Average $DD_{850\text{ mb}}$ during clear days for the irrigated ISS3 (non-irrigated ISS2) site ranged from 9.2 to 14.2 °C (9.3–12.2 °C) for the eight launch periods, with the highest $DD_{850\text{ mb}}$ being observed at the 1900 LST (0900 LST) launch time for the irrigated ISS3 (non-irrigated ISS2) site (Table 2). However, average $DD_{850\text{ mb}}$ during non-clear days for the irrigated ISS3 (non-irrigated ISS2) site ranged from 5.3 to 9.1 °C (5.0–9.4 °C) for the eight launch periods, with the highest $DD_{850\text{ mb}}$ values observed at 0500 LST (0900 LST) launch time for the irrigated ISS3 (non-irrigated ISS2) site. Overall, rawinsonde launches from over irrigated ISS3 observed a slightly lower average $DD_{850\text{ mb}}$. More moist land surface conditions under irrigation played an important role in the lower average $DD_{850\text{ mb}}$.

During clear days, average surface - 3 km lapse rates for the irrigated ISS3 site ranged between 3.5 and 7.0 °C km^{-1} with a peak during 1700 LST. Lapse rate steadily increased up to 1700 LST (Table 2). Irrigated ISS3 lapse rates are higher for most observation times compared to the lapse rates over non-irrigated ISS2 during clear days, except for 1100, 1300, and 1500 LST observations (Table 2). During non-clear days, surface - 3 km lapse rates for irrigated ISS3 ranged between 4.4 and 6.9 °C km^{-1} , peaking at 1700 LST. (Table 2). Of these, irrigated ISS3 recorded higher surface - 3 km lapse rates compared to over non-irrigated ISS2 at 0500, 0700, 1300, and 1900 LST.

Figure 6a-f shows the daytime evolution of CAPE, CIN, and 700 mb - 500 mb lapse rates for clear and non-clear days. During clear days, average CAPE for non-irrigated ISS2 ranged between 324 and 1080 J kg^{-1} where it steadily increased throughout the day and peaked at 1500 LST (Figure 6a). During non-clear days over non-irrigated ISS2, average CAPE ranged between 122 and 1374 J kg^{-1} and it was higher (up to 368) J kg^{-1} at 1700 LST) for all observation times except for 0500 LST, compared to clear days. The irrigated ISS3 observed average CAPE between 242 and 1586 J kg^{-1} during clear days and it increased throughout the day (Figure 6b). For most observation times, CAPE was higher over non-irrigated ISS2, compared to the irrigated ISS3 site during clear days except for at 1700 and 1900 LST. For non-clear days, average CAPE over irrigated ISS3 was higher (up to 388 J kg^{-1} at 1500 LST) compared to non-irrigated ISS2 for all observation periods. Overall, impacts of irrigation are evident during both clear and non-clear days.

Average CIN values for clear days and over non-irrigated ISS2 ranged between -50 and -191 J kg^{-1} and steadily increased (smaller negative value) for most of the day (Figure 6c). For most observation periods (except for 0500 and 1300 LST) average CIN over non-irrigated ISS2 was smaller (larger negative) compared to over irrigated ISS3 (Figure 6c). During non-clear days, the non-irrigated ISS2 observed average CIN values between -40 and -164 J kg^{-1} and values largely increased (smaller negative) throughout the day (Figure 6d). In addition, these values are smaller (larger negative) compared to ISS3 during non-clear days (Figure 6d). Thus, again, irrigation provided more favorable conditions for the development of convection.

During clear day morning observation times, over irrigated ISS3, average 700 mb - 500 mb lapse rates were lower compared to non-irrigated ISS2. During non-clear days, average values of 700 mb - 500 mb lapse rates for the irrigated ISS3 ranged between 6.4 and 6.8 °C km^{-1} and, generally, steadily increased throughout the day. These lapse rates for ISS3 were generally higher compared to non-irrigated ISS2 during clear days (Figure 6f) indicating favorability for convection.

3.1.3. Cloud cover and IOP

3.1.3.1. Clear days in IOP1 and IOP2.

Supplementary Table 1 shows the average LI, PWAT, $DD_{850\text{ mb}}$, and surface - 3 km lapse rates by for clear days in IOP1 and IOP2 for the eight rawinsonde launch times. During clear days in IOP1, average LI values for the irrigated ISS3 (non-irrigated ISS2) site ranged from -2.7 – -3.4 °C (-1.8 – -3.4 °C) for the eight rawinsonde launches, with the lowest LI values being observed for the 1900 LST (1300 LST) launch (Supplementary Table 1). However, during clear days in IOP2, average LI values for the irrigated ISS3 site (non-irrigated ISS2) site ranged from -3.8 – -4.3 °C (-1.8 – -4.5 °C) for the eight daily launches, with the lowest LI values observed for the 1700 and 1900 LST (1100, 1500, and 1900 LST) launches (Supplementary Table 1). Again, irrigation's influence provided a more favorable environment for development of convection.

During clear days in IOP1, the irrigated ISS3 (non-irrigated ISS2) site observed average PWAT ranged from 21.4 to 26.1 mm (23.7–27.3 mm) for the eight rawinsonde launch times (Supplementary Table 1). These values are up to 5.9 mm lower compared to the

non-irrigated ISS2 site. During clear days in IOP2, the irrigated ISS3 (non-irrigated ISS2) site observed PWAT values ranging from 29.7 to 32.5 mm (26.2–29.1 mm) for the eight rawinsonde launch times (Supplementary Table 1). In this case, over ISS3, there was up to an 11.1 mm increase in average PWAT compared to clear days in IOP1. Moreover, there was up to 6.3 mm increase in PWAT over irrigated ISS3 compared to the non-irrigated ISS2 during clear days in IOP2 indicating impacts of increased land surface moisture due to irrigation.

In the morning hours of IOP1, average surface – 3 km lapse rates were higher over non-irrigated ISS2, while higher over irrigated ISS3 in the afternoon (Supplementary Table 1). During clear days in IOP2, average surface – 3 km lapse rates were higher over irrigated ISS3 during morning and early evening (1900) observation times while they were higher over non-irrigated ISS2 during late morning and afternoon (Supplementary Table 1).

Supplementary Figure 1a-f shows the box and whisker plots of CAPE, CIN, and 700 mb – 500 mb lapse rates for clear days in IOP1 and IOP2. During clear days in IOP1, average CAPE over non-irrigated ISS2 ranged from 308 to 1401 J kg⁻¹ for the previously noted observation times (Supplementary Figure 1a). Irrigated ISS3 observed higher CAPE compared to non-irrigated ISS2 during early morning (0500 and 0700 LST) and early evening hours (1900 LST) during IOP1. During clear days in IOP2, irrigated ISS3 observed higher CAPE in the afternoon and evening hours (Supplementary Figure 1b).

Average CIN for clear days in IOP1 for the irrigated ISS3 ranged between –10 and –175 J kg⁻¹ and CIN values generally increased (smaller negative) through the day (Supplementary Figure 1c). For most of the day irrigated ISS3 observed lower (larger negative value) CIN compared to ISS2. Again, during clear days in IOP2, average CIN over irrigated ISS3 was higher (smaller negative value) during early morning and early afternoons (Supplementary Figure 1d).

During clear days in IOP1, average 700 mb – 500 mb lapse rates over non-irrigated ISS2 trended slightly higher or equal compared to ISS3 during afternoon and early evening. On the other hand, during clear days in IOP2, irrigated ISS3 observed higher average lapse rates compared to non-irrigated ISS2 during afternoon and early evening. Overall, all three measures capture impacts of irrigated land use on (increased) favorability of development of convection.

3.1.3.2. Non-clear days in IOP1 and IOP2. Supplementary Table 2 shows the average LI, PWAT, DD_{850 mb}, and surface – 3 km lapse rates for non-clear days in IOP1 and IOP2 for each rawinsonde launch times. During non-clear days in IOP1, average LI values for the irrigated ISS3 (non-irrigated ISS2) site ranged from –5.2–0.3 °C (-5.3–1.5 °C) during the eight launches (per day), with the lowest LI values being observed from 0900 to 1700 LST (1100–1500 LST) launch times (Supplementary Table 2). However, during non-clear days in IOP2, average LI for the irrigated ISS3 (non-irrigated ISS2) ranged from –4.9–0.8 °C (-4.2–3.5 °C) for the eight launches, with the lowest LI values being observed at the 1500 and 1700 LST (1700 LST) launch times.

Average PWAT values for the irrigated ISS3 (non-irrigated ISS2) site ranged from 26.1 to 30.9 mm (27.4–33.0 mm) during non-clear days in IOP1, and the highest average PWAT value was observed at 1500 LST (1900 LST) (Supplementary Table 2). During non-clear days in IOP2, average PWAT values ranged from 33.8 to 35.4 mm (33.2–35.9 mm) (Supplementary Table 2). The highest PWAT value was observed at 1700 LST (1500 LST) for the irrigated ISS3 (non-irrigated ISS2).

For IOP1 and non-clear days, average DD_{850 mb} over irrigated ISS3 was generally smaller compared to non-irrigated ISS2 during mid-morning through late afternoon while the opposite is true for early morning and early evening observations. Overall, the average DD_{850 mb} is smaller over both irrigated and non-irrigated land use during IOP2, which is the peak growing season for crops. However, for five out of eight observations times DD_{850 mb} was smaller over irrigated land use (ISS3) [compared to non-irrigated land use (ISS2)] pointing towards the impact of irrigation.

Supplementary Figure 2a-f shows the box and whisker plots of CAPE, CIN, and 700 mb – 500 mb lapse rates for non-clear days in IOP1 and IOP2. During non-clear days in IOP1, average CAPE over irrigated ISS3 ranged between 589 and 1822 J kg⁻¹ and it steadily increased throughout the day (Supplementary Figure 2a). These values are higher compared to over non-irrigated ISS2, except for observations at 1300 and 1500 LST. During non-clear days in IOP2, average CAPE over irrigated ISS3 was noticeably higher (up to 878 J kg⁻¹) compared to over non-irrigated ISS2 for observation times between 1300 and 1500 LST, indicating favorable influence of irrigated land use on convective environment (Supplementary Figure 2b).

During non-clear days in IOP1, average CIN values were smaller (larger negative) over irrigated ISS3 in the morning and gradually became larger (smaller negative) through late afternoon suggesting environment was more conducive for convective development (Supplementary Figure 2c). During non-clear days in IOP2, the average CIN was more conducive to convection over irrigated areas compared to non-irrigated, in the morning and mid- and late-afternoon.

During non-clear days in IOP1, average 700 mb – 500 mb lapse rates were greater over irrigated ISS3. Five of eight observation times recorded higher average 700 mb – 500 mb lapse rates (up to 0.6 °C km⁻¹) over irrigated area (ISS3). In addition, the differences (irrigated vs. non-irrigated) are greater in the morning soundings with slightly higher values over irrigated land use. During non-clear days in IOP2, for seven of eight observation times irrigated ISS3 recorded higher average 700 mb – 500 mb lapse rates (up to 0.3 °C km⁻¹) compared to over non-irrigated land use, suggesting more instability over irrigated areas and potentially favorable condition for convection development.

Overall, timing of maximum averages changed with cloud cover. For example, during clear days, the irrigated ISS3 and non-irrigated ISS2 reported maximum average CAPE of 1586 J kg⁻¹ and 1080 J kg⁻¹, respectively, at 1900 and 1500 LST. However, during non-clear days, irrigated ISS3 and non-irrigated ISS2 observed maximum average CAPE of 1749 J kg⁻¹ and 1374 J kg⁻¹, respectively, both at 1700 LST (Table 2). In other words, during clear days, the irrigated ISS3 site observed a maximum average CAPE which is 163 J kg⁻¹ higher and occurred two hours earlier compared to non-clear days. While the non-irrigated ISS2 site experienced the maximum average CAPE two hours later for clear days but it was 294 J kg⁻¹ higher compared to non-clear days.

Environmental lapse rates play an important role in convective environments (Carlson et al., 1983; Doswell et al., 1985; Craven and Brooks, 2004) and so does precipitable water (Salby, 1996). For most cases, the irrigated sites tend to have higher surface – 3 km lapse rates during the early morning hours (0500, 0700 LST, for example) and early evening hours (1900 LST) compared to the non-irrigated sites. During non-clear days in IOP2, the irrigated ISS3 site had higher 700 – 500 mb lapse rates than the non-irrigated ISS2 site for the 0500, 0700, 0900, 1100, 1500, and 1700 LST launch times (Supplementary Figure 2 f). The higher lapse rates, for these respective times in lower and mid-troposphere throughout the growing season, suggests more favorable conditions for convective development over irrigated areas and thus influence of land use and land cover.

During IOP2 when irrigation peaks, the irrigated site had higher average PWAT compared to the non-irrigated sites during clear days. Again, increased soil moisture and moist land surface hydrologic conditions, and higher latent heat flux played a role in the higher PWAT over irrigated ISS3. During non-clear days in IOP2, average PWAT values were higher for the irrigated sites during the morning hours only. A combination of higher CAPE, PWAT, and lapse rates for irrigated (non-irrigated) land use during the morning and evening (afternoon) hours suggest a more favorable environment for convection over irrigated (non-irrigated) land use during those times.

To further understand the findings of this research, results were assessed in the context of the theoretical understanding of the role of soil moisture/land surface hydrology and land-atmosphere interactions under irrigation. A framework which uses Convective Triggering Potential (CTP), and Low-Level Humidity Index (HI_{low}) was created to determine location for convective initiation as it relates to the surface energy balance and soil moisture (Findell and Eltahir, 2003a, b). This framework was successfully used alongside the LCL Deficit to assess convective environments over irrigated and non-irrigated cropland using GRAINEX data (Whitesel et al., 2024b). The LCL deficit is the difference between the LCL and the planetary boundary layer height (PBLH). Under moist or wetter land surface conditions and higher latent heat flux (i. e., in this case human modified land surface hydrology), the LCL deficit would be lower and provide favorable conditions for cloud formation. Previously, results from Whitesel et al. (2024b) and Lachenmeier et al. (2024) suggested that irrigation and resulting increase in soil moisture and higher latent heat flux would impact the convective environment, which further supports findings of the current research.

This paper and Rappin et al. (2021) report that with increasing applications of irrigation and as growing season progresses from early to peak, a binary switch like change in soil moisture occurs. Binary switch is characterized by shifting from absence or limited applications of irrigation to rapidly increased and extensive applications of irrigation where soil moisture increases rapidly due to increased irrigation (Fig. 4). It has been found that CTP, HI_{low} and LCL deficits decrease with this binary switch. Based on the CTP- HI_{low} framework (Findell and Eltahir, 2003a), it can be suggested that increasing irrigation influenced convective environments via modified heat and moisture fluxes when growing season shifted from IOP1 to IOP2. Again, results of the current study agree with the past studies.

Several previous GRAINEX studies have been dedicated to the analysis of the daytime evolution of the PBL and the effects of L-A interactions on convective environments (Rappin et al., 2021, 2022; Phillips et al., 2022; Lachenmeier et al., 2024; Whitesel et al., 2024a, b). L-A interactions are significantly influenced by land surface hydrologic conditions such as soil moisture and latent and sensible heat flux (which are also dependent on soil moisture content). Applications of irrigation increase soil moisture and increase (decrease) latent (sensible) heat flux (Figs. 4 and 5) (Rappin et al., 2021, 2022; Lachenmeier et al., 2024). This shift in heat flux contributes to the moistening of the PBL and planetary boundary layer height (PBLH) is reduced as a result (Rappin et al., 2022; Lachenmeier et al., 2024). As noted previously, LCL and LFC have been found to be decreased with the application of irrigation, increased soil moisture and increased latent heat flux (Lachenmeier et al., 2024). Together they can present a favorable condition for convection development. In other words, the results of this study are generally in agreement with previous findings. It also needs to be noted that the current study provides bi-hourly evolution of daytime convective environment based on observed data and convective diagnostic variables, which were absent from past studies and thus a valuable contribution in scientific literature.

In a related study, Brooke et al. (2023) also noted that irrigation (i.e., increased soil moisture and latent heat flux) substantially impacted the development of the boundary layer and the morning transition. They have found that the mean buoyancy flux was 2.8 times smaller over irrigated land use compared to rainfed/arid land use during morning transition. They observed a 30- to 90-minute delay in the near-surface buoyancy-flux crossover time over irrigated land use. Hence, through these changes irrigated land use can also alter potential timing of convection, as found in the current study. Recently, Wang et al. (2024) noted that under wet soil conditions boundary layer moisture could be sufficient to generate the required buoyancy profiles for afternoon precipitation events. Greve et al. (2025) found that irrigated land use caused increases in downwind afternoon precipitation. Thus, findings of the present research and other studies (e.g., Wang et al., 2024) provide further insights in understanding the mechanisms and pathways for irrigation related convection and precipitation. In short, for all of these cases, irrigation, enhanced soil moisture, and the resulting changes in various moisture and heat fluxes led to modification of the convective environments.

Finally, the results can assist local and regional weather forecasters. They can add irrigation impacts in the forecasting metrics, which could potentially improve weather forecasts. Such improvements can assist local populations in a variety of decision making including short and long-term hydrological managements. The latter two management decisions could include near-term irrigation applications, reservoir management, river forecasting etc. The improvements in these management decisions eventually will also help with efficient use of water resources in the region.

4. Concluding remarks

Land use land cover change (LULCC) plays a significant role in affecting the weather, climate, and hydrology. Irrigated agriculture is one of the most notable examples of LULCC. It changes soil moisture and the surface energy balance in such a way that it favors

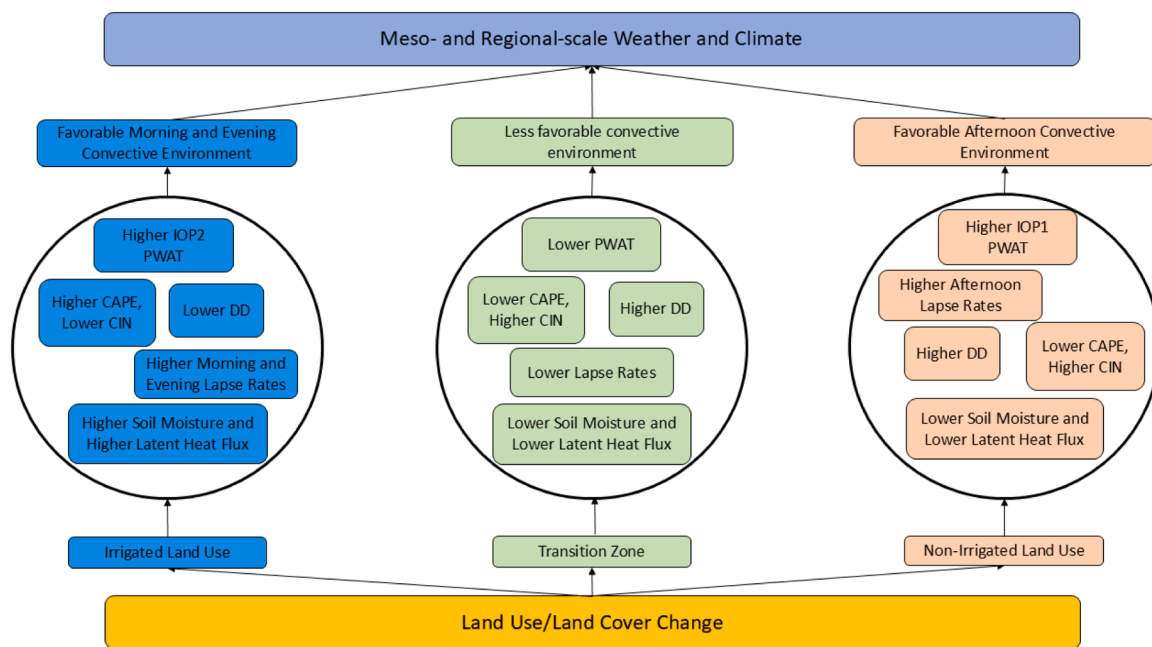


Fig. 7. Land use land cover change, irrigation, modified land surface hydrologic condition, and their impacts on the daytime evolution of the convective environment.

higher latent heat flux over lower sensible heat flux, and changes albedo, moisture flux, convective environment, cloud development, and precipitation, among others. Despite apparent stability brought on by irrigation due to surface cooling, the increase in soil moisture and latent heat flux in contrast to the drier soils in non-irrigated areas can create a favorable environment for development of convection.

It was found that irrigated land use featured higher CAPE and lower CIN compared to the non-irrigated and transitional land use. Irrigated land use resulted in higher PWAT during clear days and in the mornings, late afternoons and evenings, while the non-irrigated land use observed higher PWAT during the afternoons and on non-clear days. Additionally, environmental lapse rates were found to be higher during morning and evening observations for irrigated land use during clear days and for the non-irrigated land use during afternoons of non-clear days. Thus, based on the analyses using storm diagnostic variables, irrigated land use promotes a more favorable convective environment during the morning and evening hours, while the non-irrigated land use supports a more favorable convective environment during the afternoon hours. Fig. 7 further summarizes the findings of this study.

Overall, this study shows the importance of conducting future research focusing on the impacts of irrigated land use on nocturnal convective environments. Nocturnal convection is difficult to understand since there is a lack of solar forcing to support surface-based processes. Irrigation also provides excess residual moisture that can be utilized for nighttime or morning convection. Thus, a field data collection campaign and subsequent research focusing on both nocturnal and daytime hours need to be pursued. This type of research, dedicated to the study of evolution of nocturnal convective environment over irrigated areas, would further complete our understanding of its impacts. Similar types of field data collection campaign and research for other major irrigated areas can be also undertaken to better understand irrigation impacts on meso- and regional-scale weather and climate.

CRedit authorship contribution statement

Daniel Whitesel: Writing – original draft, Visualization, Validation, Methodology, Investigation, Formal analysis, Data curation. **Rezaul Mahmood:** Writing – review & editing, Writing – original draft, Validation, Supervision, Resources, Project administration, Methodology, Investigation, Funding acquisition, Formal analysis, Conceptualization. **Eric Rappin:** Writing – review & editing, Funding acquisition. **Paul Flanagan:** Writing – review & editing, Methodology, Formal analysis. **Chris Phillips:** Writing – review & editing, Methodology. **Pielke Roger:** Writing – review & editing, Methodology, Funding acquisition. **Udaysankar Nair:** Writing – review & editing, Funding acquisition.

Declaration of Competing Interest

The authors declare that they have no known competing financial interests or personal relationships that could have appeared to influence the work reported in this paper.

Acknowledgments

The authors would like to thank the Editor-in-Chief, Associate Editor, and two anonymous reviewers for their valuable feedback. This research is funded by the National Science Foundation (NSF) Grants AGS-1853390 (Rezaul Mahmood and Eric Rappin), AGS-1720477 (Udaysankar Nair), and AGS-1552487 (Roger Pielke Sr.). Mention of trade names or commercial products in this publication is solely for the purpose of providing specific information and does not imply recommendation or endorsement by the U.S. Department of Agriculture. USDA is an equal opportunity provider and employer.

Appendix 1. List of acronyms

CAPE Convective Available Potential Energy
 CTP Convective Triggering Potential
 CIN Convective Inhibition
 DD_{850 mb} Dewpoint Depression
 DOW6 Doppler on Wheels 6
 DOW7 Doppler on Wheels 7
 DOW8 Doppler on Wheels 8
 EMESH Environmental Monitoring Economical Sensor Hubs
 GRAINEX Great Plains Irrigation Experiment
 GP-LLJ Great Plains Low-Level Jet
 ISFS Integrated Surface Flux System
 IOP1 Intense Observation Period 1; Early Growing Season
 IOP2 Intense Observation Period 2; Peak Growing Season
 ISS2 Integrated Sounding System 2
 ISS3 Integrated Sounding System 3
 L-A Land-Atmosphere
 LCL Lifting Condensation Level
 LFC Level of Free Convection
 LI Lifted Index
 HI_{low} Low-Level Humidity Index
 LULCC Land Use Land Cover Change
 PBL Planetary Boundary Layer
 PBLH Planetary Boundary Layer Height
 PWAT Precipitable Water
 SM-P Soil Moisture-Precipitation

Appendix A. Supporting information

Supplementary data associated with this article can be found in the online version at [doi:10.1016/j.ejrh.2025.102884](https://doi.org/10.1016/j.ejrh.2025.102884).

Data availability

Data will be made available on request.

References

- Barstorn, A., Schickedanz, P.T., 1984. The effect of irrigation on warm season precipitation in the Southern Great Plains. *J. Clim. Appl. Meteor.* 23, 865–888.
- Brooke, J.K., Best, M.J., Locke, A.P., Osborne, S.R., Price, J., Cuxart, J., Boone, A., Canut-Rocafort, G., Hartogensis, O.K., Roy, A., 2023. Irrigation contrasts through the morning transition. *Q. J. R. Meteorol. Soc.* 150 (758), 170–194. <https://doi.org/10.1002/qj.4590>.
- Brooks, H.E., 2007. Ingredients Based Forecasting. In: Gaiotti, D.B., Steinacker, R., Stel, F. (Eds.), *Atmospheric Convection. Research and Operational Forecasting Aspects*, 475. CISM International Centre for Mechanical Sciences, Springer, Vienna. https://doi.org/10.1007/978-3-211-69291-2_12.
- Carlson, T.N., Benjamin, S.G., Forbes, G.S., Li, Y.F., 1983. Elevated mixed layers in the regional severe storm environment: Conceptual model and case studies. *Mon. Wea. Rev.* 111, 1453–1473.
- Colby, F.P., 1984. Convective inhibition as a predictor of convection during AVE-SESAME II. *Mon. Wea. Rev.* 112, 2239–2252. [https://doi.org/10.1175/1520-0493\(1984\)112<2239:CIAAPO>2.0.CO;2](https://doi.org/10.1175/1520-0493(1984)112<2239:CIAAPO>2.0.CO;2).
- Collow, T.W., Robock, A., Wu, W., 2014. Influences of soil moisture and vegetation on convective precipitation forecasts over the United States Great Plains. *J. Geophys. Res. Atmos.* 119, 9338–9358. <https://doi.org/10.1002/2014JD021454>.
- Cook, B.I., McDermid, S.S., Puma, M.J., Williams, A.P., Seager, R., Kelley, M., Nazarenko, L., Aleinov, I., 2020. Divergent regional climate consequences of maintaining current irrigation rates in the 21st century. *J. Geophys. Res.* 125, e2019JD031814. <https://doi.org/10.1029/2019JD031814>.
- Cook, B.I., Puma, M.J., Krakauer, N.Y., 2011. Irrigation induced surface cooling in the context of modern and increased greenhouse gas forcing. *Clim. Dyn.* 37, 1587–1600.

- Cook, B.I., Shukla, S.P., Puma, M.J., Nazarenko, L.S., 2015. Irrigation as an historical climate forcing. *Clim. Dyn.* 44, 1715–1730. <https://doi.org/10.1007/s00382-014-2204-7>.
- Craven, J.P., Brooks, H.E., 2004. Baseline climatology of sounding derived parameters associated with deep moist convection. *Natl. Wea. Dig.* 28, 13–24.
- DeAngelis, A., Dominguez, F., Fan, Y., Robock, A., Kustu, M.D., Robinson, D., 2010. Evidence of enhanced precipitation due to irrigation over the Great Plains of the United States. *J. Geophys. Res.* 115 (D15115). <https://doi.org/10.1029/2010JD013892>.
- Doswell, C.A., III, H.E., Brooks, Maddox, R.A., 1996. Flash flood forecasting: an ingredients-based methodology. *Wea. Forecast.* 11, 560–581. [https://doi.org/10.1175/1520-0434\(1996\)011<0560:FFFAIB>2.0.CO;2](https://doi.org/10.1175/1520-0434(1996)011<0560:FFFAIB>2.0.CO;2).
- Doswell, C.A., III, F., Caracena, Magnano, M., 1985. Temporal evolution of 700–500-mb lapse rate as a forecasting tool—A case study. *Preprints. 14th Conf. Sev. Local Storms Indianap. Am. Meteor. Soc.* 398–401.
- Eltahir, E.A., 1998. A soil moisture–rainfall feedback mechanism: 1. Theory. *Obs. Water Res. Res.* 34, 765–776.
- Fan, X., Ma, Z., Yang, Q., Han, Y., Mahmood, R., Zheng, Z., 2015a. Land use/land cover changes and regional climate over the Loess Plateau during 2001–2009 – Part I. Observed evidences. *Clim. Change* 129, 427–440. <https://doi.org/10.1007/s10584-014-1069-4>.
- Fan, X., Ma, Z., Yang, Q., Han, Y., Mahmood, R., 2015b. Land use/land cover changes and regional climate over the Loess Plateau during 2001–2009 – Part II. Interrelationship from observations. *Clim. Change* 129, 441–455. <https://doi.org/10.1007/s10584-014-1068-5>.
- Findell, K.L., Eltahir, E.A.B., 2003a. Atmospheric controls on soil moisture–boundary layer interactions. Part I: Framework development. *J. Hydrometeorol.* 4, 552–569.
- Findell, K.L., Eltahir, E.A.B., 2003b. Atmospheric controls on soil moisture–boundary layer interactions. Part II: Feedbacks within the continental United States. *J. Hydrometeorol.* 4, 570–583.
- Frye, J.D., Mote, T., 2010a. Convection initiation along soil moisture boundaries in the Southern Great Plains. *Mon. Wea. Rev.* 138, 1140–1151. <https://doi.org/10.1175/2009MWR2865.1>.
- Frye, J.D., Mote, T.L., 2010b. The synergistic relationship between soil moisture and the low-level jet and its role on the prestorm environment in the Southern Great Plains. *J. Appl. Meteor. Clim.* 49, 775–791. <https://doi.org/10.1175/2009JAMC2146.1>.
- Galway, J.G., 1956. The lifted index as a predictor of latent instability. *Bull. Am. Meteor. Soc.* 43, 528–529.
- Greve, P., Schmitt, A.U., Miralles, D.G., McDermid, S., Findell, K.L., García-García, A., Peng, J., 2025. Observational evidence of increased afternoon rainfall downwind of irrigated areas. *Nat. Comm.* 16, 3415. <https://doi.org/10.1038/s41467-025-58729-y>.
- Holt, T.R., Niyogi, D., Chen, F., Manning, K., LeMone, M.A., Qureshi, A., 2006. Effect of land–atmosphere interactions on the IHOP 24–25 May 2002 convection case. *Mon. Wea. Rev.* 134, 113–133.
- Hu, Q., Achugbu, I.C., Chen, L., 2024. Irrigation effects on regional circulation and climate in the U.S. Great Plains: A case study. *J. Clim.* 37, 6549–6562.
- Lachenmeier, E., Mahmood, R., Phillips, C., Nair, U., Rappin, E., Pielke Sr., R.A., W., Oncley, Brown, Wurman, S., Kosiba, J., Kaulfus, K., Santanello, A., Jr, J., Kim, E., Lawston-Parker, P., Hayes, M., Franz, T.E., 2024. Irrigated agriculture significantly modifies seasonal boundary layer atmosphere and lower-tropospheric convective environment. *J. Appl. Meteor. Clim.* 63, 245–262. <https://doi.org/10.1175/JAMC-D-23-0020.1>.
- Lanucci, J.M., 1985. An operational procedure using elevated mixed-layer analyses to predict severe-storm outbreaks. *Preprints. 14th Conf. Sev. Local Storms Indianap. Am. Meteor. Soc.* 406–409.
- Lanucci, J.M., Warner, T.T., 1991a. A synoptic climatology of the elevated mixed-layer inversion over the southern Great Plains in Spring. Part 1: Structure, dynamics, and seasonal evolution. *Wea. Forecast.* 6, 181–197.
- Lanucci, J.M., Warner, T.T., 1991b. A synoptic climatology of the elevated mixed-layer inversion over the southern Great Plains in Spring. Part 2: The life cycle of the lid. *Wea. Forecast.* 6, 198–213.
- Lanucci, J.M., Warner, T.T., 1991c. A synoptic climatology of the elevated mixed-layer inversion over the southern Great Plains in Spring. Part 3: Relationship to severe-storms climatology. *Wea. Forecast.* 6, 214–226.
- Lewis, W., 1957. Forecasting 700-mb. dewpoint depression by a 3-dimensional trajectory technique. *Mon. Wea. Rev.* 85, 297–301. [https://doi.org/10.1175/1520-0493\(1957\)085<0297:FMDDBA>2.0.CO;2](https://doi.org/10.1175/1520-0493(1957)085<0297:FMDDBA>2.0.CO;2).
- Mahmood, R., Foster, S.A., Keeling, T., Hubbard, K.G., Carlson, C., Leeper, R., 2006. Impacts of irrigation on 20th century temperature in the Northern Great Plains. *Glob. Planet. Change* 54, 1–18.
- Mahmood, R., Hubbard, K.G., 2002. Anthropogenic land-use change in the North American tall grass-short grass transition and modification of near-surface hydrologic cycle. *Clim. Res.* 21, 83–90.
- Mahmood, R., Hubbard, K.G., Carlson, C., 2004. Modification of growing season surface temperature records in the Northern Great Plains due to land use transformation: verification of modeling results and implication for global climate change. *Int. J. Clim.* 24, 311–327.
- Mahmood, R., Keeling, T., Foster, S.A., Hubbard, K.G., 2013. Did irrigation impact 20th century temperature in the High Plains aquifer region? *Appl. Geogr.* 38, 11–21.
- Mahmood, R., Littell, A., Hubbard, K.G., You, J., 2012. Observed data-based assessment of relationships among soil moisture at various depths, precipitation, and temperature. *Appl. Geogr.* 34, 255–264.
- Mahmood, R., Pielke Sr., R.A., Hubbard, K.G., Niyogi, D., Bonan, G., Lawrence, P., Baker, B., McNider, R., McAlpine, C., Etter, A., Gameda, S., Qian, B., Carleton, A., Beltran-Przekurat, A., Chase, T., Quintanar, A.I., Adegoke, J.O., Vezhapparambu, S., Conner, G., Asefi, S., Sertel, E., Legates, D.R., Wu, Y., Hale, R., Frauenfeld, O. N., Watts, A., Shepherd, M., Mitra, C., Anantharaj, V.G., Fall, S., Lund, R., Nordfelt, A., Blanken, P., Du, J., Chang, H.-I., Leeper, R., Nair, U.S., Dobler, S., Deo, R., Syktus, J., 2010. Impacts of land use land cover change on climate and future research priorities. *Bull. Am. Meteor. Soc.* 91, 37–46.
- Mahmood, R., Pielke, R.A., Hubbard, K.G., Niyogi, D., Dirmeyer, P.A., McAlpine, C., Carleton, A.M., Hale, R., Gameda, S., Beltrán-Przekurat, A., Baker, B., McNider, R., Legates, D.R., Shepherd, M., Du, J., Blanken, P.D., Frauenfeld, O.W., Nair, U.S., Fall, S., 2014. Land cover changes and their biogeophysical effects on climate. *Inter. J. Climatol.* 34, 929–953.
- May, R.M., Arms, S.C., Marsh, P., Bruning, E., Leeman, J.R., Goebbert, K., Thielen, J.E., Bruick, Z., Camron, M.D., 2024. MetPy: A Python Package for Meteorological Data. *Unidata Unidata/MetPy v1.6* [Softw.]. <https://doi.org/10.5065/D6WW7G29>.
- May, R.M., Goebbert, K.H., Thielen, J.E., Leeman, J.R., Camron, M.D., Bruick, Z., Bruning, E.C., Manser, R.P., Arms, S.C., Marsh, P.T., 2022. MetPy: A Meteorological Python Library for Data Analysis and Visualization. *Bull. Am. Meteor. Soc.* 103, E2273–E2284. <https://doi.org/10.1175/BAMS-D-21-0125.1>.
- McDermid, S.M., Nocco, Lawston-Parker, P., Keune, J., Pokhrel, Y., Jain, M., Jägermeyr, J., Brocca, L., Massari, C., Jones, A., Vahmani, A., P., Thiery, W., Yao, Y., Bell, A., Chen, L., Dorigo, W., Hanasaki, N., Jasechko, J., Min-Hui, Lo, Mahmood, R., Mishra, V., Mueller, N.D., Niyogi, D., Rabin, S., Sam, S., Sloat, L., Wada, Y., Zappa, L., Chen, F., Cook, B.I., Kim, H., Lombardozi, D., Polcher, J., Ryu, D., Santanello, J., Satoh, Y., Seneviratne, S., Singh, D., Yokohata, T., 2023. Irrigation in the Earth system. *Nat. Rev. Earth Environ.* <https://doi.org/10.1038/s43017-023-00438-5>.
- McDermid, S.S., Mahmood, R., Hayes, M., Bell, J.E., Lieberman, Z., 2021. Environmental trade-offs for sustainable irrigation. *Nat. Geosci.* 14, 706–709.
- McPherson, R., 2007. A review of vegetation–atmosphere interactions and their influences on mesoscale phenomena. *Progr. Phys. Geogr.* 31, 261–285.
- Moncrieff, M.W., Miller, M.J., 1976. The Dynamics and Simulation of Tropical Cumulonimbus and Squall Lines. *Q. J. R. Meteorol. Soc.* 102 (432), 373–394. <https://doi.org/10.1002/qj.49710243208>.
- Ozdogan, M., Gutman, G., 2008. A new methodology to map irrigated areas using multi-temporal MODIS and ancillary data: An application example in the continental US. *Remote Sens. Env.* 112, 3520–3537.
- Paccini, L., Schiro, K.A., 2025. Influence of soil moisture on the development of organized convective systems in South America. *J. Geophys. Res.* 130, e2024JD042108.
- Parsons, D., Dabberdt, W., Cole, H., Hock, T., Martin, C., Barrett, A.L., Miller, E., Spowart, M., Howard, M., Ecklund, W., Carter, D., 1994. The integrated sounding system: description and preliminary observations from TOGA COARE. *Bull. Am. Meteor. Soc.* 75 (4), 553–567. [https://doi.org/10.1175/1520-0477\(1994\)075%3C0553:TISSDA%3E2.0.CO;2](https://doi.org/10.1175/1520-0477(1994)075%3C0553:TISSDA%3E2.0.CO;2).
- Pei, L., Moore, N., Zhong, S., Kendall, A.D., Gao, Z., Hyndman, D.W., 2016. Effects of irrigation on summer precipitation over the United States. *J. Clim.* 29, 3541–3558.

- Phillips, C.E., Nair, U.S., Mahmood, R., Rappin, E., Pielke Sr., R.A., 2022. Influence of irrigation on diurnal mesoscale circulations: results from GRAINEX. *Geophys. Res. Lett.* 49, e2021GL096822.
- Pielke, R.A., 2001. Influence of the spatial distribution of vegetation and soils on the prediction of cumulus convective rainfall. *Rev. Geophys.* 39, 151–177.
- Pielke, R.A., Mahmood, R., McAlpine, C., 2016. Land's complex role in climate change. *Phys. Today* 69, 40–46.
- Pielke Sr., R.A., Pitman, A., Niyogi, D., Mahmood, R., McAlpine, C., Hossain, F., Klein Goldewijk, K., Nair, U., Betts, R., Fall, S., Reichstein, M., Kabat, P., de Noblet-Ducoudré, N., 2011. Land use/land cover changes and climate: Modeling analysis and observational evidence. *Wiley Inter. Rev. Clim. Change* 2, 828–850.
- Pielke, R.A., Zeng, X., 1989. Influence on severe storm development of irrigated land. *Nat. Wea. Dig.* 14, 16–17.
- Rappin, E., Mahmood, R., Nair, U., Pielke Sr., R.A., Brown, W., Oncley, S., Wurman, J., Kosiba, K., Kaulfus, C., Phillips, E., Lachenmeier, J., Santanello, E., Kim, P., Lawston-Parker, 2021. The Great Plains Irrigation Experiment (GRAINEX). *Bull. Am. Meteor. Soc.* 102, ES1756–ES1785.
- Rappin, E.D., Mahmood, R., Nair, U.S., Pielke Sr., R.A., 2022. Land-atmosphere interactions during GRAINEX: planetary boundary layer evolution in the presence of irrigation. *J. Hydrometeorol.* 23, 1401–1417.
- Salby, M.L., 1996. *Fundamentals of Atmospheric Physics*. Academic Press, p. 627.
- Santanello Jr., J.A., Dirmeyer, P.A., Ferguson, C.R., Findell, K.L., Tawfik, A.B., Berg, A., Ek, M., Gentine, P., Guillod, B.P., van Heerwaarden, C., Roundy, J., Wulfmeyer, V., 2018. Land–atmosphere interactions: The LoCo perspective. *Bull. Am. Meteor. Soc.* 99, 1253–1272.
- Schultz, P., 1989. Relationships of Several Stability Indices to Convective Weather Events in Northeast Colorado. *Wea. Forecast.* 4, 73–80. [https://doi.org/10.1175/1520-0434\(1989\)004<0073:ROSSIT>2.0.CO;2](https://doi.org/10.1175/1520-0434(1989)004<0073:ROSSIT>2.0.CO;2).
- Sen Roy, S., Mahmood, R., Niyogi, D.D.S., Lei, M., Foster, S.A., Hubbard, K.G., Douglas, E., Pielke Sr., R.A., 2007. Impacts of the agricultural Green Revolution induced land use changes on air temperatures in India. *J. Geophys. Res.* 112, D21108. <https://doi.org/10.1029/2007JD008834>.
- Sen Roy, S., Mahmood, R., Quintanar, A., Gonzalez, A., 2011. Impacts of irrigation on dry season precipitation in India. *Theor. Appl. Clim.* 104, 193–207.
- Storm Prediction Center, 2024. Sounding Analysis Help Page. Accessed 11 April 2024. (<https://www.spc.noaa.gov/exper/soundings/help/index.html>).
- Szilagy, J., Franz, T.E., 2020. Anthropogenic hydrometeorological changes at a regional scale: observed irrigation–precipitation feedback (1979–2015) in Nebraska, USA. *Sustain. Water Resour. Manag.* 6, 1. <https://doi.org/10.1007/s40899-020-00368-w>.
- Taylor, C., de Jeu, R., Guichard, F., Harris, P., Dorigo, W., 2012. Afternoon rain more likely over drier soils. *Nature* 489, 1476–1487.
- Taylor, C.M., Prigent, C., Dadson, S.J., 2018. Mesoscale rainfall patterns observed around wetlands in sub-saharan africa. *Q. J. R. Meteorol. Soc.* 144, 2118–2132.
- Thompson, R., 2006. Explanation of SPC Severe Weather Parameters. Storm Prediction Center. Accessed 6 February 2024. (<https://www.spc.noaa.gov/exper/mesoanalysis/help/begin.html>).
- UCAR/NCAR - Earth Observing Laboratory, 1997. NCAR Integrated Sounding System (ISS). Accessed February 19, 2024. <https://doi.org/10.5065/D6348HF9>.
- Wang, G., Fu, R., Zhuang, Y., Dirmeyer, P.A., Santanello, J.A., Wang, Gu, Yang, K., McColl, K., 2024. Influence of lower-tropospheric moisture on local soil moisture–precipitation feedback over the US Southern Great Plains. *Atmos. Chem. Phys.* 24, 3857–3868.
- Whitesel, D., Mahmood, R., Flanagan, P., Rappin, E., Nair, U., Pielke Sr., R.A., Hayes, M., 2024a. Impacts of irrigation on a precipitation event during GRAINEX in the High Plains Aquifer region. *Agric. For. Meteorol.* 345 (2024), 1–21. <https://doi.org/10.1016/j.agrformet.2023.109854>.
- Whitesel, D., Mahmood, R., Roundy, J., Phillips, C., Rappin, E., Flanagan, P., Santanello, J., Nair, U., Pielke Sr., R.A., 2024b. Assessing convective environment over irrigated and non-irrigated land uses with land-atmosphere coupling metrics: results from GRAINEX. *J. Hydrometeorol.* 25, 1061–1080.
- Whitesel, D., Mahmood, R., Flanagan, P., Phillips, C., Nair, U., Pielke Sr., R.A., Rappin, E., 2025. Impacts of irrigated and non-irrigated land use on convective environments and related diagnostic variables during GRAINEX in Nebraska, USA. *J. Hydrometeorol.* 26, 501–519.
- Wurman, J., Kosiba, K., Pereira, B., Robinson, P., Frambach, A., Gilliland, A., White, T., Aikins, J., Trapp, R.J., Nesbitt, S., Hanshaw, M.N., Lutz, J., 2021. The Flexible Array of Radars and Mesonets (FARM). *Bull. Am. Meteor. Soc.* 102, E1499–E1525. <https://doi.org/10.1175/BAMS-D-20-0285.1>.
- Xu, Z., Mahmood, R., Yang, Z.-L., Fu, C., Su, H., 2015. Investigating diurnal and seasonal climatic response to land use and land cover change over monsoon Asia with the Community Earth System Model. *J. Geophys. Res.* 120, 1137–1152. <https://doi.org/10.1002/2014JD022479>.